

Control of DFIG for improvement of voltage regulation in a power system using recurrent neural networks

Ali Asghar Shojaei*, Mohd Fauzi Othman, Rasoul Rahmani, Masoud Samadi

Centre for Artificial Intelligence and Robots, Universiti Teknologi Malaysia, 54100 Kuala Lumpur, Malaysia
Shojaei2012@gmail.com

Abstract: This article focuses on the voltage control of Doubly Fed Induction Generator (DFIG) wind turbines using Recurrent Neural Network (RNN). The paper also compares the performance of Static Synchronous Compensator (STATCOM) and DFIG systems, subject to the line to ground fault. The RNN is used in two main parts which are RNN Identifier (RNNI) and RNN Controller (RNNC). Performance of the DFIG is simulated and analyzed with and without the RNN controller. In this study, voltage regulation on Recurrent Neural Network is designed to control for a standard multi-machine power system. The results demonstrated significant improvement in the voltage regulation using the RNN controller for DFIG in the power system.

[Ali Asghar Shojaei, Mohd Fauzi Othman, Rasoul Rahmani, Masoud Samadi. **Control of DFIG for improvement of voltage regulation in a power system using recurrent neural networks.** *Life Sci J* 2013;10(12s):761-769]. (ISSN:1097-8135). <http://www.lifesciencesite.com>. 122

Keyword: Recurrent neural network, control, DFIG, voltage regulation, STATCOM

1. Introduction

Nowadays, power systems play important roles in human's life. Reliability and stability of such systems are vital issues in power engineering. A fault occurrence in transmission lines may lead to damages in power equipments or consumer devices. Therefore, control of sudden load changes or fault occurrence in a power system is essential [1].

Today, different types of induction generators are used in wind energy technology. The two major types are fixed speed and variable speed generators. Variable speed equipment includes wind production in which the wind turbine power coefficient is optimum for the general use of the speed collection. The two common types of wind turbine are DFIG and synchronous generator which are driven by generators converter [2]. DFIG has a rotor winding which changes voltage source coupled to slip rings of the rotor. The stator winding is related in a straight line to the network and the rotor winding is associated with the network via an electronic power regulator. In [3], a detailed description is presented to show how a DFIG works. For constancy studies, network scheming of a DFIG should be taken into consideration in the dynamic analysis of a serious disturbance [4].

In the past, wind turbines were primarily used to protect the system from the poor performance of the turbine oriented and impact of the functioning on the network, because the penetration of wind turbine was very low. However, this situation has changed dramatically, and achieved high penetration of wind energy [5]. Independent of providing electrical energy, it is as well essential to contribute in voltage regulation.

Some scientific studies have been dedicated to challenges in proliferation of wind energy. The function has no negative influence on the stability of a small network. The study in [6] is focused on the variable speed turbines which can improve the transient stability near conservative power plants. It is suggested in [7] that some types of wind turbines may participate in the energy vibration.

By increasing the penetration of wind energy, some requirements are defined for the wind turbines connectivity requirements to the grid. The requirements are different around the world and are related to issues such as expansion, preservation and operation in synchronized, dependability and effectiveness [8-10]. The voltage control is compulsory, especially for the cases that the power system includes DFIG and STATCOM systems.

This article proposes the use of wind DFIG controlled by RNN to improve voltage regulation of integrated utilities. The RNN is utilized in two parts including RNN Identifier (RNNI) and RNN Controller (RNNC). The RNNI's function is detecting irregular outputs of power system plant through a feedback mechanism. The RNNC's function is controlling and regulating outputs of power system. The results demonstrate that by applying the new control strategy for integrated systems, stability of voltage regulation can be improved significantly.

The structure of this paper is as follows. In section 2, recurrent neural network control strategy is presented. Section 3 contains power system model. Voltage regulation approaches is explained in section 4. In section 5, power system simulation is introduced. In addition, the results analysis to explained in section 6. Finally, the paper is concluded in Section 7.

2. Recurrent neural network (RNN) control strategy

At first, RNN is aimed to the contra wise dynamics via the system with noticing output-input of data, and ponder cyclic contains a repeated internal, external and three layers comprising of layer neurons also hidden layer neurons and one output layer adjustment opinions organization and all other nodes in the same level of cross.

The main difference between the RNN and the feed-forward neural network is having several feedback loops. In this study, every RNN system consists of a Recurrent Neural Network Controller (RNNC) and a Recurrent Neural Network Identifier (RNNI). Here, RNNI makes a sample of the plant which is being controlled, and the feedback is sent to RNNC for creating the control signal. In Fig. 1 schematic block diagram of the applied RNN is shown.

Neural network (NN), frequently in the form of rings, different feedback, compared with only one-loop feed-forward NN. These will be NN Control $G_c(s)$ RNNC (s) and RNNI $\tilde{G}_p(s)$ as exposed in Fig. 1[11].

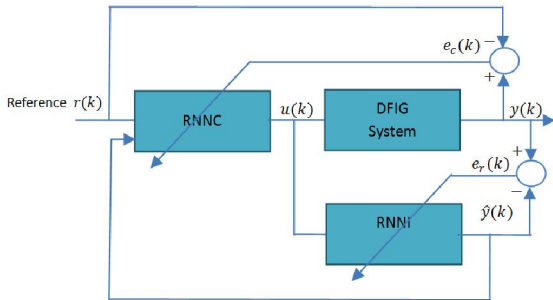


Fig. 1. RNNI and RNNC using IMC.

2.1 Recurrent neural network identifier (RNNI)

The structure of the RNNI part is depicted in Figure. 2. Here the applied model is a two layered network with output and input layers [12, 13] with each one having m_1 and n_1 neurons respectively. In Figure 2, $I_{j1}(t)$ and $O_{j1}(t)$ are the input and output of j^{th} neuron of the input layer respectively, while the input and output of the k^{th} neuron of output layer are denoted as $I_{k2}(t)$ and $O_{k2}(t)$. In addition, $u(t)$, $x_1(t-1)$, $x_2(t-1)$, $x_3(t-1)$ and $x_4(t-1)$ are considered as the inputs of RNNI. Note that in all the equations superscripts 1 and 2 correspond to the input and output layers respectively. $W_{ji}^R(t)$ and $W_{kj}^O(t)$ are the recurrent weights which connect the neurons together. $W_{ji}^R(t)$ connects the neurons of the input layer and $W_{kj}^O(t)$ determines the factors for connections between neurons of the output layer [14, 15].

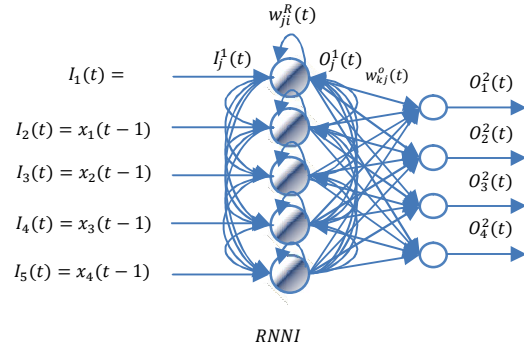


Fig. 2. The RNNI structure

The RNNI form is as follows:

Input- output layer of the j th neuron:

$$I_j^1(t) = I_j(t) + \sum_{i=1}^{m_1} W_{ji}^R(t) \times O_i^1(t-1), j = 1, \dots, m_1 \tag{1}$$

$$O_j^1(t) = f(I_j^1(t)) = \frac{e^{I_j^1(t)} - e^{-I_j^1(t)}}{e^{I_j^1(t)} + e^{-I_j^1(t)}}, j = 1, \dots, m_1 \tag{2}$$

Input-output layers of the k th neuron:

$$O_k^2(t) = I_k^2(t) = \sum_{i=1}^{m_1} w_{ki}^O(t) O_j^1(t), k = 1, \dots, n_1 \tag{3}$$

Error function:

$$E_1(t) = \frac{1}{2} \sum_{k=1}^{n_1} (X_k(t) - O_k^2(t))^2 \tag{4}$$

$x_k(t)$, $k = 1, \dots, n_1$, are the outputs.

Weights $W_{kj}^O(t)$ and $W_{ji}^R(t)$ are determined using the steepest decline algorithms with the following equations:

$$W_{kj}^O(t+1) = W_{kj}^O(t) + \Delta W_{kj}^O(t) = W_{kj}^O(t) - \eta_l^O \frac{\partial E_1(t)}{\partial W_{kj}^O(t)} \tag{5}$$

$$W_{ji}^R(t+1) = W_{ji}^R(t) + \Delta W_{ji}^R(t) = W_{ji}^R(t) - \eta_l^R \frac{\partial E_1(t)}{\partial W_{ji}^R(t)} \tag{6}$$

$E_1(t)$ is expressed as:

$$\frac{\partial E_1(t)}{\partial W_{kj}^O(t)} = (X_k(t) - O_k^2(t)) O_j^1(t) \tag{7}$$

$$\frac{\partial E_1(t)}{\partial W_{ji}^R(t)} = -\sum_{k=1}^{n_1} [(X_k(t) - O_k^2(t)) W_{kj}^O(t) (-O_j^1(t))] O_j^1(t-1) \tag{8}$$

2.2 Recurrent neural network controller (RNNC)

The other important part of a RNN is RNNC which is shown in Figure. 3. RNNC contains two layers which are the output and input layers. Here, we include m_c neurons for the input layer and only one neuron for the output layer. $S_j^1(t)$ and $T_j^1(t)$ determine the output-input of j^{th} neuron of the input layer respectively. Alike RNNI, we have five inputs for the RNNC which are $u(t-1)$, $x_1(t-1)$, $x_2(t-1)$, $x_3(t-1)$ and $x_4(t-1)$. As stated before, the output layer has only a single neuron which has the input and output of $S_2(t)$ and $u(t)$ respectively. Note that $u(t)$ is the same signal which is considered as the control signal. The recurrent weights, which connect the input and output of the neurons, are $V_{ji}^R(t)$ and $V_j^O(t)$ for the input and output layers respectively. The output and input layers of the j^{th} neuron are determined by the following formula:

$$S_j^1(t) = S_j(t) + \sum_{i=1}^{m_c} V_{ji}^R(t) T_i^1(t-1), j = 1, \dots, m_c \tag{9}$$

$$T_j^1(t) = f(S_j^1(t)) = \frac{e^{S_j^1(t)} - e^{-S_j^1(t)}}{e^{S_j^1(t)} + e^{-S_j^1(t)}}, j = 1, \dots, m_1 \tag{10}$$

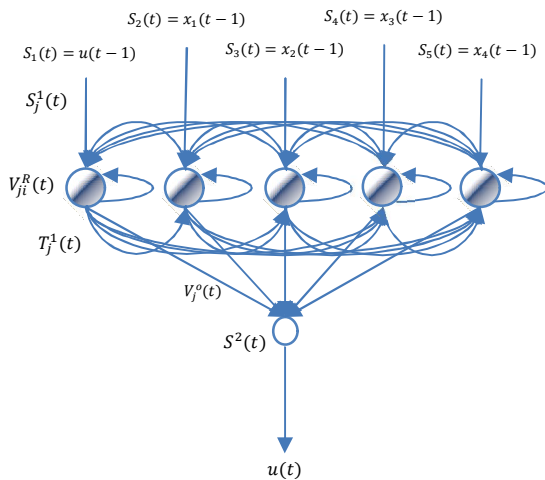


Fig. 3. The RNNC arrangement.

Output single is indicated as follows:

$$u(t) = S^2(t) = \sum_{j=1}^{m_c} V_j^O(t) T_j^1(t) \tag{11}$$

Error function:

$$E_c(t) = \frac{1}{2} \sum_{k=1}^{m_c} (r_k(t) - x_k(t))^2 \tag{12}$$

The position is $r_k(t)$, $k = 1, \dots, m_c$.

$V_{ji}^R(t)$ and $V_{kj}^R(t)$ resolute by:

$$V_j^O(t+1) = V_j^O(t) + \Delta V_j^O(t) = V_{kj}^O(t) - \frac{\partial E_c(t)}{\partial V_j^O(t)} \tag{13}$$

$$V_{ji}^R(t+1) = V_{ji}^R(t) + \Delta V_{ji}^R(t) = V_{ji}^R(t) - \eta_c^R \frac{\partial E_c(t)}{\partial V_{ji}^R(t)} \tag{14}$$

So, η_c^R and η_c^O are gradient errors with respect to the weights $V_j^O(t)$ and $V_{ji}^R(t)$ are:

$$\frac{\partial E_c(t)}{\partial V_j^O(t)} = - \sum_{k=1}^{m_c} [(r_k(t) - x_k(t)) W_{kj}^O(t) (1 - (O_j^1(t))^2)] T_j^1(t) \tag{15}$$

$$\frac{\partial E_c(t)}{\partial V_{ji}^R(t)} = - \sum_{k=1}^{m_c} [(r_k(t) - x_{kj}(t)) W_{kj}^O(t) (1 - (O_j^1(t))^2)] \tag{16}$$

3. Power system model

In this study, a multi machine Kundur model is used with the structure illustrated in Figure 4. As shown in the figure, the model consists of two large areas. Each area consists of two 900 MVA machines. The two areas are coupled by a 220kv double circuit line of 220km length. Each area has a 187Mvar capacitors. The system has been modeled and simulated in Matlab / Simulink software. Here, STATCOM and DFIG are controlled by RNN at bus 12, separately.

The system [16] is used to track the transient performance of the proposed controller.

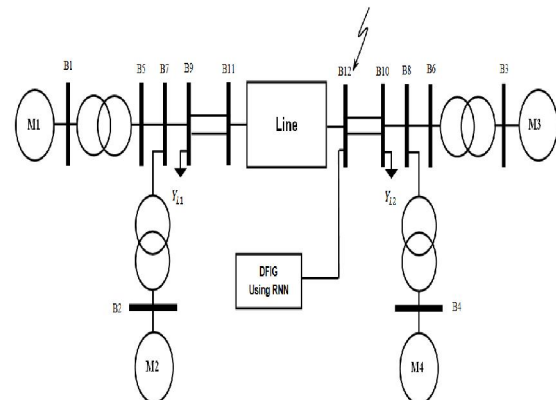


Fig. 4. Block diagram of the test system

4. Voltage regulation approaches

4.1 Voltage regulation using STATCOM

The FACTS devices such as STATCOM, increase power systems stability using their ability to provide

and support the performance during faults [17, 18]. STATCOM provides reactive power for the system. The output from the control loop separately regulates the injection of the reactive power and the voltage at the DC bus of the STATCOM, and the control circuit generates an internal voltage reference [19]. In other words, the output current can be maintained substantially independent from the AC system. Reactive power generation or absorption varies linearly with the supply voltage. Figure 5 shows a typical STATCOM system.

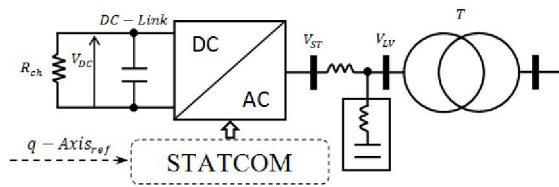


Fig. 5. The structure of STATCOM

Usually STATCOM is suitable for supporting the power network when the power factor is poor. On the other hand, FACTS devices, especially STATCOM are very expensive. Improving the stability of the power system is one of the most difficult tasks for STATCOM.

4.2 Voltage regulating using DFIG

By increasing the penetration of wind energy especially in countries where wind speed is high, the first problem emerges is a low voltage output on the side connected to the network during a fault. Secondly, it may affect the loads close to the wind turbine by dropping their voltage. The major problem is that the drops in the supply voltage can threaten the local area as well. In recent years, some adjustable voltage networks have got worldwide attention. Usually, the control voltage at the supply bus, which is connected to the grid, is performed based on the desired active power and reactive power injected or absorbed.

The regulation capacity of the reactive power in a wind power plant is a natural consequence of the continuation of interaction between the network and the wind turbine. So, there are a number of problems regarding the voltage control of DFIG turbines in a power plant. The wind energy alternates in nature and that in reason of difficulties in voltage regulation of DFIG [20].

Nowadays, the DFIG wind turbines are highly recommended in the industry [21, 22]. This type of wind turbines offers high-potential output with a small size power converter. DFIG wind turbine need a proper

control system to supply a portion of the load demand in the grid [23]. Moreover, for a small size power converter installed, the amount of capacitive power is quite less than it is active power to be delivered; hence, it is often necessary to install additional reactive compensation system. DFIG can have a keen control on the reactive power where it can deliver a high amount to the grid or absorb it by itself.

The DFIG uses a variable speed system; connected in full control on the generator reactive power and the rotor frequency (see Figure 6).

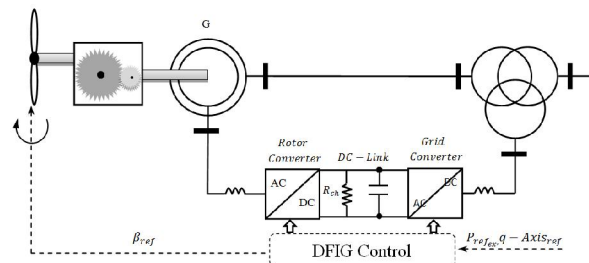


Fig. 6. The structure of doubly fed generator induction

This contributes to the dynamic performance of the DFIG model, see the description below which refers to the analysis presented in [24]:

- Pitch control, mechanical power provided to regulate the property of the shaft;
- Electrical generation properties of converter on the rotor side;
- Electrical control includes provides, regulating in active and reactive, as well as mechanical angle.

4.3. Voltage regulating using DFIG by RNN control

This part provides a comprehensive description about the control of DFIG using RNN. The effectiveness of the DFIG control using RNN is analyzed and compared to STATCOM and DFIG under different fault conditions. The response time for the DFIG controlled by RNN control is another interesting point of discussion during the fault. During the system disturbances, using the RNN control system energizes the generator to inject reactive power to the grid. Normally, the role of the controller is to enable the highest possible power for each wind speed based on the pitch structure for assurance that the revolving speed of the generator is enough for power generation.

As explained, the presented control system is based on RNN. The block diagram of the whole control system is shown in Fig. 7. In addition, the proposed DFIG control provides minimum reactive power injection to grid.

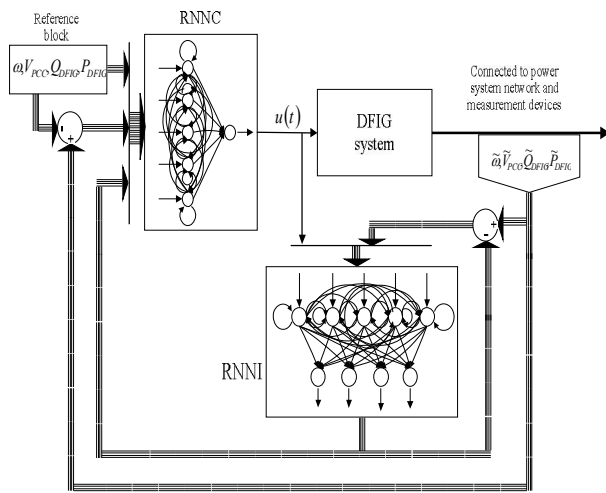


Fig. 7. The complete block diagram of DFIG control system.

Where, the input signals to the RNN are as follows:

- : the measured frequency from the Point of Common Coupling (PCC) in per-unit;
- V_{pcc} : the measured voltage at the PCC in per-unit;
- Q_{DFIG} : the measured reactive power to be injected to the PCC by DFIG in per-unit;
- P_{DFIG} : the measured active power to be received from the PCC by DFIG in per-unit.

5. Power system simulation

Since the proposed method is applied for the first time to such a system, several types of test cases are designed to show the feasibility and capability of the RNN control system. Since the main idea of using a DFIG in a power system is to regulate the voltage level, the most important graph in all the test cases is the voltage versus time graph.

In the next part, the power system simulation results are presented. The results contain bus voltage regulation plot, active power plot and generator's speed plot. Although the main goal of this study is voltage regulation, the other plots are presented as the supplementary result of the simulations. In the results, voltage regulation is related to voltage of bus No.12 in Figure 4 and the active power is the transmitted power from bus No.11 to bus No.12.

The simulated RNNI and RNNC models in MATLAB/Simulink GUI environment are presented in Figures 8 and 9. As shown in the figures, three different parts have been designed in each model containing the input, output and weight matrix parts.

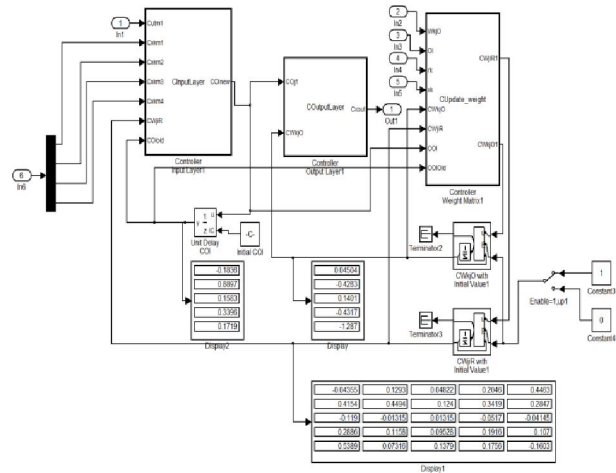


Fig. 8. The contents of the RNN controller block.

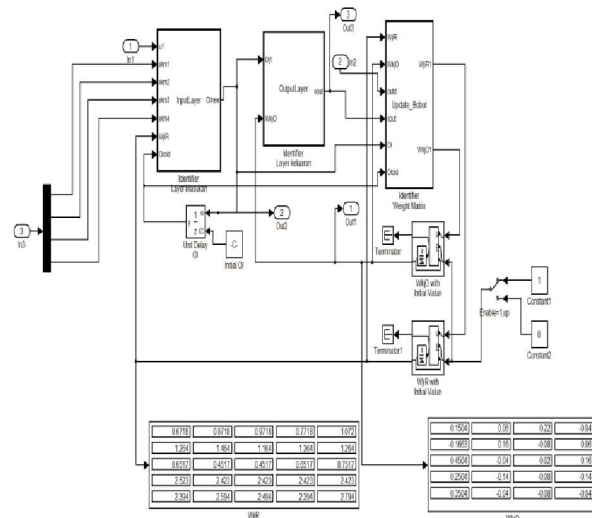


Fig. 9. The contents of the RNN identifier block.

5.1 STATCOM voltage regulation simulation

In this section, performance of the power system model using STATCOM has been presented. In the simulation, a single phase fault on the bus STATCOM occurs, the term is applied for 0.08 seconds. The effect of the fault on speed of the generator and voltage of the bus is shown in Figure 10 to 12. As seen in the figures, the voltages at STATCOM bus, active power and speed of generators are completely controlled.

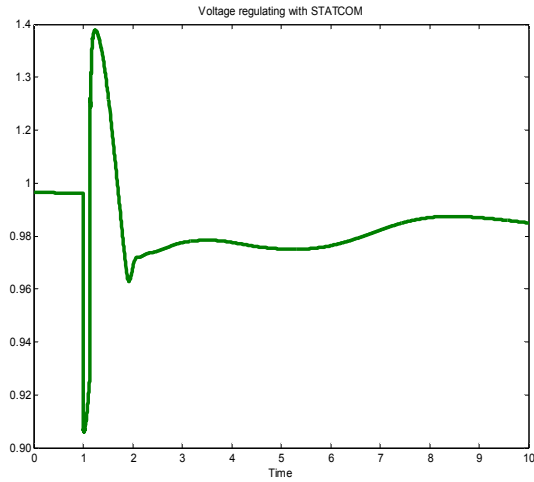


Fig.10. Voltage regulating using STATCOM

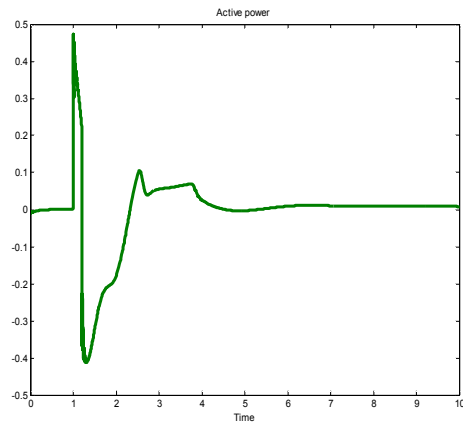


Fig.11.Active power using STATCOM

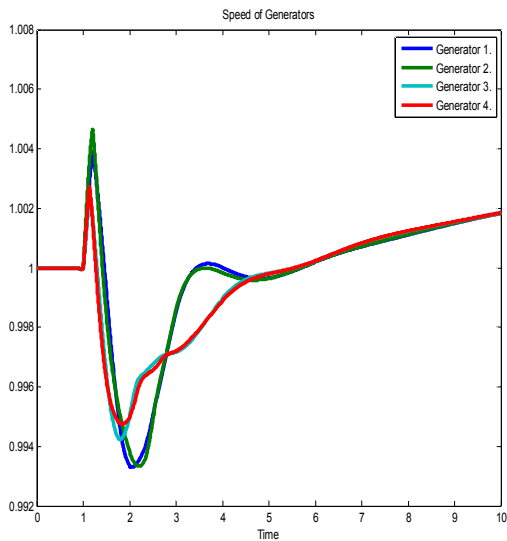


Fig.12. Speed of generators using STATCOM.

5.2 DFIG voltage regulation simulation

In this part, the power system performance has been analyzed using DFIG voltage regulation. For this purpose, the power system is simulated again under fault occurrence condition similar to the previous subsection. The difference is only using the DFIG instead of the STATCOM. Figures 13 to 15 demonstrate the voltage regulation, active power and speed of generators, respectively.

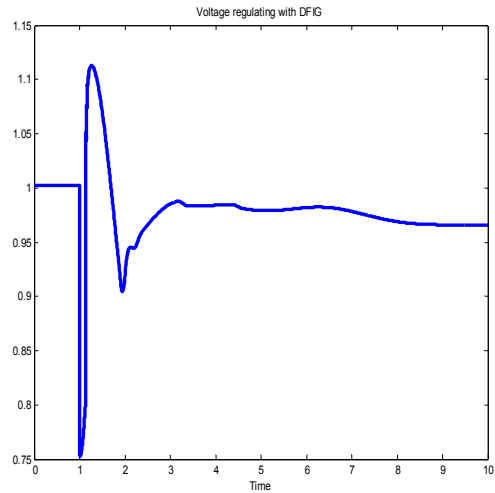


Fig.13. Voltage regulating using DFIG

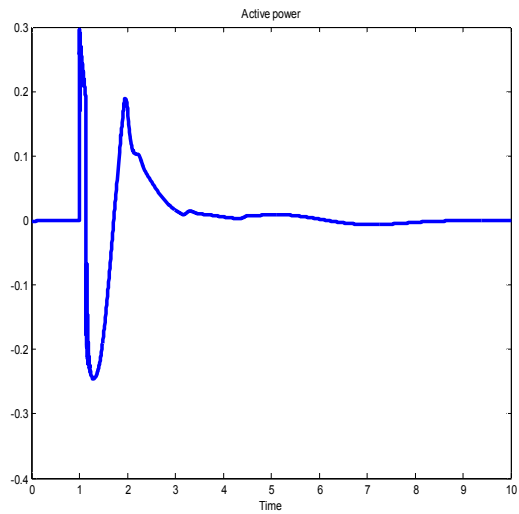


Fig.14. Active power using DFIG

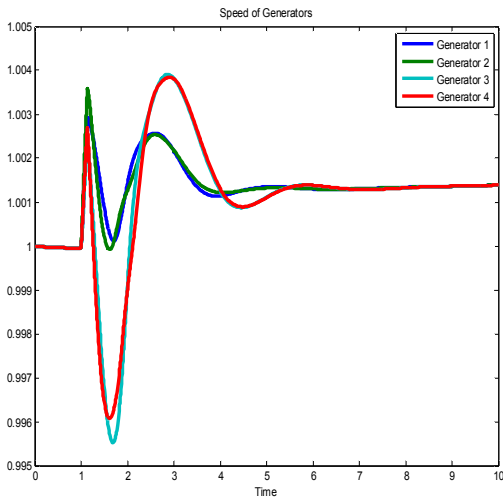


Fig.15. Speed of generators using DFIG

5.3 DFIG voltage regulation simulation using RNN

In this part, the power system performance using DFIG has been simulated again. The difference between this section and the previous one is the use of RNN for DFIG control. The RNN has been utilized here because of the variations in wind speed which affects the DFIG performance. In Figure 16, variations of wind speed in a certain time period is illustrated.

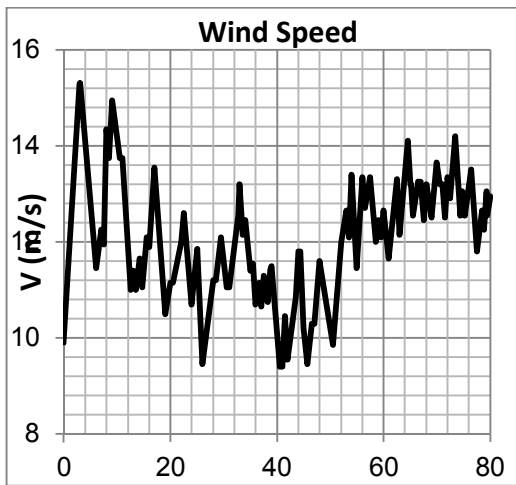


Fig.16. Variations of wind speed in a time period [25]

Figures 17 to 19 demonstrate the voltage regulation, active power and speed of generators for this case, respectively.

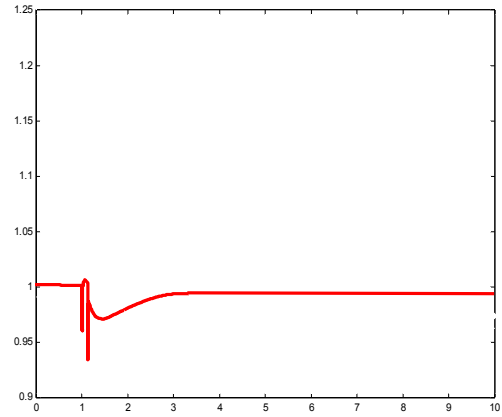


Fig.17 .Voltage regulation using RNN

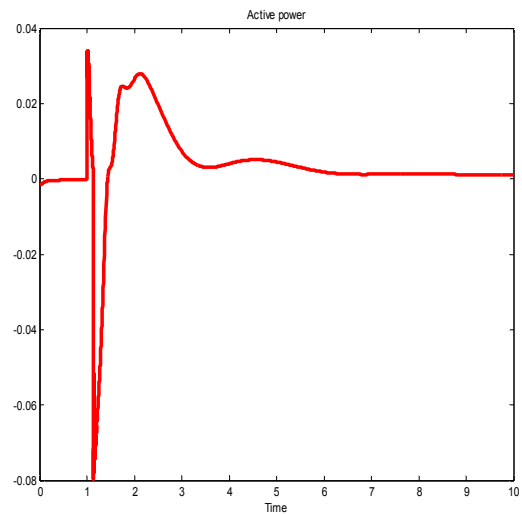


Fig.18 .Active power using RNN

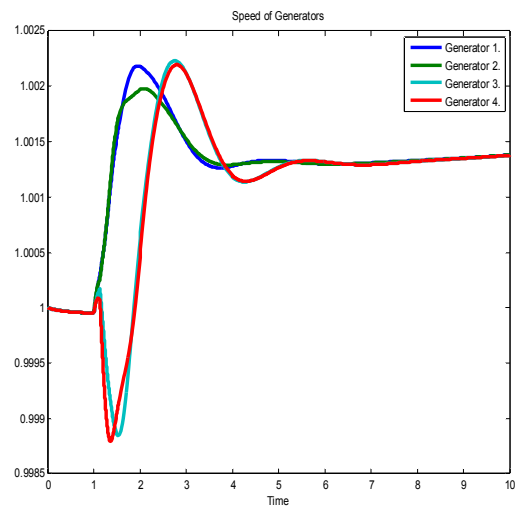


Fig.19. Speed of generators using RNN

6. Results and analysis

In the previous section, the voltage regulation, active power and generator speed plots were presented under three different conditions. The plots are quantitatively analyzed in this section. Table 1, states overshoot, rise time, steady state error and settling time parameters for different cases.

Table 1. The results of simulation

	STATCOM	DFIG	DFIG control using RNN
Over Shot % (OS)	39.59	12.07	1.23
Rise Time (t_r)	0.11 ms	0.08 ms	0.032 ms
Error steady state	0.015 v	0.035 v	0.008 v
Time Settling (t_s)	6.85 s	6.17 s	2.68 s

In control theory, overshoot refers to an output exceeding its final steady state value. For increasing the facilities life time and avoiding shock to the systems, it is supposed to decrease the overshoot in transient response. In STATCOM the overshoot percentage is %39.59. In DFIG, the overshoot percentage is %12.07 which is better than STATCOM and acceptable for the system. But the best overshoot percentage is for DFIG control using RNN which is %1.23. It is much less than the other overshoot results. This comparison shows that the last controller has the best performance in overshoot parameter. The rise time for these three control strategies are also different. For STATCOM and DFIG rise times are 0.11ms and 0.08ms respectively but DFIG using RNN has the lowest rise time equal to 0.032 ms which is much faster than the others.

The third factor of step response that was studied in this work is steady state error. The steady-state error is the difference between the reference input and the output when the time goes to infinity. The most accurate system between these three is DFIG using RNN that has the less steady state error equal to 0.008 V. After that STATCOM with 0.015 V has better accuracy than DFIG with 0.035 V steady state errors. The last factor in Table 1 is settling time that is the time after which the signal stays within the tolerance value +/- 2%. The settling times for STATCOM and DFIG are 6.85s and 6.17s. But for DFIG using RNN is 2.68s that is much less than the others.

All in all, RNN gives the utmost rate control of varying DFIG voltage bus during fault for voltage regulating and decrease the active power to grid, so it can be effectively implemented based on the principle of reasoning.

7. Conclusion

In this article a RNN controller is developed to enhance voltage regulation in a power system using DFIG. The performance of the DFIG control using RNN is analyzed and compared with STATCOM and DFIG under fault conditions. The effectiveness of the proposed controller was evaluated during fault in the large area, via power system simulation. The simulation results demonstrate that using the RNN approach, voltage regulation can be enhanced while the active power and generators speed responses are also improved.

Acknowledgment

The authors would like to thank the Ministry of Higher Education of Malaysia (MOHE), the Universiti Teknologi Malaysia and Centre for Artificial Intelligence and Robotics (CAIRO) for their supports.

References

1. J. Machowski, J. Bialek, and J. Bumby, Power system dynamics: stability and control: Wiley, 2011.
2. Shafiu, O. Anaya-Lara, G. Bathurst, and N. Jenkins, "Aggregated wind turbine models for power system dynamic studies," Wind engineering, vol. 30, pp. 171-185, 2006.
3. K. Clark, N. W. Miller, and J. J. Sanchez-Gasca, "Modeling of ge wind turbine-generators for grid studies," General Electric International inc. One River Road Schenectady, NY April, vol. 16, 2010.
4. Arief, Z. Dong, M. B. Nappu, and M. Gallagher, "Under voltage load shedding in power systems with wind turbine-driven doubly fed induction generators," Electric Power Systems Research, vol. 96, pp. 91-100, 2013.
5. J. M. Morales, A. J. Conejo, and J. Pérez-Ruiz, "Economic valuation of reserves in power systems with high penetration of wind power," Power Systems, IEEE Transactions on, vol. 24, pp. 900-910, 2009.
6. F. Dong, B. H. Chowdhury, M. L. Crow, and L. Acar, "Improving voltage stability by reactive power reserve management," Power Systems, IEEE Transactions on, vol. 20, pp. 338-345, 2005.
7. Avramovic and L. Fink, "Real-time reactive security monitoring," in Power Industry Computer Application Conference, 1991. Conference Proceedings, 1991, pp. 373-378.

8. H. Golpîra, H. Bevrani, and A. H. Naghshbandy, "An approach for coordinated automatic voltage regulator–power system stabiliser design in large-scale interconnected power systems considering wind power penetration," *Generation, Transmission & Distribution, IET*, vol. 6, pp. 39-49, 2012.
9. R. Sebastián and R. P. Alzola, "Effective active power control of a high penetration wind diesel system with a Ni–Cd battery energy storage," *Renewable Energy*, vol. 35, pp. 952-965, 2010.
10. S. Sreedharan, W. Ongsakul, J. Singh, K. Buayai, and I. Wartana, "PSO based tuning of FACTS controllers for maximizing the wind energy penetration in power systems," in *Innovative Smart Grid Technologies-India (ISGT India)*, 2011 IEEE PES, 2011, pp. 287-293.
11. R. Rahmani, A. A. Shojaei, M. F. Othman, and R. Yusof, "Novel Control System for VAR Compensator Using Recurrent Neural Network to Improve Voltage Regulation " *Electrical Engineering 2013*.
12. C.-J. Chen and T.-C. Chen, "Design of a power system stabilizer using a new recurrent neural network," in *Innovative Computing, Information and Control, 2006. ICICIC'06. First International Conference on*, 2006, pp. 39-43.
13. J. He and O. Malik, "An adaptive power system stabilizer based on recurrent neural networks," *Energy Conversion, IEEE Transactions on*, vol. 12, pp. 413-418, 1997.
14. Shojaei, M. Othman, R. Rahmani, and M. Rani, "Implementation of Recurrent Neural Network to Control Rotational Inverted Pendulum using IMC Scheme," *Australian Journal of Basic and Applied Sciences*, vol. 6, pp. 299-306, 2012.
15. Shojaei, M. Othman, R. Rahmani, and M. Rani, "A Hybrid Control Scheme for a Rotational Inverted Pendulum," in *Computer Modeling and Simulation (EMS), 2011 Fifth UKSim European Symposium on*, 2011, pp. 83-87.
16. P. Kundur, N. J. Balu, and M. G. Lauby, *Power system stability and control vol. 4: McGraw-hill New York*, 1994.
17. Hammad, "Analysis of power system stability enhancement by static var compensators," *Power Systems, IEEE Transactions on*, vol. 1, pp. 222-227, 1986.
18. H. Tyll, "FACTS technology for reactive power compensation and system control," in *Transmission and Distribution Conference and Exposition: Latin America, 2004 IEEE/PES, 2004*, pp. 976-980.
19. Y.-H. Song and A. T. Johns, *Flexible ac transmission systems (FACTS): Inst of Engineering & Technology*, 1999.
20. J. Kennedy, B. Fox, and D. Morrow, "Distributed generation as a balancing resource for wind generation," *Renewable Power Generation, IET*, vol. 1, pp. 167-174, 2007.
21. E. MUHANDO, "Modeling-based design of intelligent control paradigms for modern wind generating systems," *University of the Ryukyus*, 2008.
22. R. Doherty, A. Mullane, G. Nolan, D. J. Burke, A. Bryson, and M. O'Malley, "An assessment of the impact of wind generation on system frequency control," *Power Systems, IEEE Transactions on*, vol. 25, pp. 452-460, 2010.
23. W. Qiao, R. G. Harley, and G. K. Venayagamoorthy, "Coordinated reactive power control of a large wind farm and a STATCOM using heuristic dynamic programming," *Energy Conversion, IEEE Transactions on*, vol. 24, pp. 493-503, 2009.
24. Rahman, "Fuzzy logic based improved Active and Reactive Power control operation of DFIG for Wind Power Generation," *ICPE 2011-ECCE Asia*, 654~ 661 쪽 (총 8 쪽), 2011.
25. J. Shi, Y. J. Tang, L. Ren, J. D. Li, and S. J. Chen, "Application of SMES in wind farm to improve voltage stability," *Physica C: Superconductivity*, vol. 468, pp. 2100-2103, 9/15/ 2008.

12/12/2013